energies

MDPI

Article

Effectiveness of Automatic Disconnection of Supply in the Islandable TN–C Household Electrical Installation Equipped with Photovoltaic Source and Battery Energy Storage System

Roman Korab [1], Mirosław Kiełboń [1], Paweł Kubek [1,*], Andrzej Latko [2], Krzysztof Maźniewski [1], Bernard Witek [1], Dominik Duda [1], Agnieszka Dziendziel [1], Henryk Kocot [1] and Tomasz Rusek [1]

[1] Department of Power Systems and Control, Faculty of Electrical Engineering, Silesian University of Technology, 44-100 Gliwice, Poland; roman.korab@polsl.pl (R.K.); miroslaw.kielbon@polsl.pl (M.K.); krzysztof.mazniewski@polsl.pl (K.M.); bernard.witek@polsl.pl (B.W.); dominik.duda@polsl.pl (D.D.); agnieszka.dziendziel@polsl.pl (A.D.); henryk.kocot@polsl.pl (H.K.); tomasz.rusek@polsl.pl (T.R.)
[2] Department of Power Electronics, Electrical Drives and Robotics, Faculty of Electrical Engineering, Silesian University of Technology, 44-100 Gliwice, Poland; andrzej.latko@polsl.pl
* Correspondence: pawel.kubek@polsl.pl

Abstract

Photovoltaic sources and energy storage are increasingly being installed in power supply systems of residential buildings. As a result, consumer installations are being transformed into prosumer installations, typically operating as grid-connected, but often also with the option of island operation. Legally binding standards specify the technical requirements that an islandable prosumer electrical installation (PEI) must meet, including those regarding shock protection. Unfortunately, when older installations, constructed in accordance with the then-current standards, are converted into PEI systems, these requirements are not always met. This raises the question of the safety of users operating islandable PEIs that do not meet up-to-date requirements. The aim of this paper is to assess the effectiveness of shock protection in the case of indirect contact (automatic disconnection of supply—ADS) in various operating modes of the reference islandable PEI constructed in the TN–C earthing system, i.e., incompatible with current standards. First, the effectiveness of ADS was assessed using commonly applied calculation and measurement methods. Contrary conclusions were obtained for island operation modes of the reference PEI. Therefore, to verify the effectiveness of the ADS, measurements of short-circuit currents and touch voltage waveforms were taken during actual short circuits. The obtained results confirm that the requirements for protection against electric shock in case of indirect contact (ADS) were met in all operating modes of the analyzed PEI.

Keywords: electric shock; indirect contact; automatic disconnection of supply; TN–C earthing system; islandable prosumer electrical installation; photovoltaic source; battery energy storage system

Academic Editor: Philippe Leclère

Received: 14 October 2026
Revised: 17 November 2026
Accepted: 24 November 2026
Published: 27 November 2026

Copyright: © 2026 by the authors. Licensee MDPI, Basel, Switzerland. This article is an open access article distributed under the terms and conditions of the Creative Commons Attribution (CC BY) license.

1. Introduction

In today's world, electricity is the second dominant form of energy used in the residential sector in EU countries [1]. It covers over 25% of final energy consumption in residential buildings, ensuring the functioning of electrical appliances used in households. However, in some situations, it can pose a serious threat to human health and life. This

can happen as a result of electric shock [2]. Therefore, it is necessary to use adequate technical measures to minimize the risk of such a situation occurring. All the solutions used in this area create an electric shock protection system [3]. From the point of view of the subject of this article, the shock protection system used in household electrical installations is of special interest.

In the case of a home electrical installation, electric shock can generally occur in two situations: as a result of contact with a live part (this is the so-called direct contact), or as a result of touching an exposed conductive part (ECP) that has become live as a result of a fault (this is the so-called indirect contact) [4]. The currently applicable international standard IEC 60364 [5] specifies the protective measures against electric shock that must be taken in both situations. In the case of protection against direct contact, the most frequently applied method of protection is the basic insulation of live parts. In the case of protection against indirect contact (fault protection), the standard recommends several measures, the first of which is automatic disconnection of supply (ADS) with an operating time depending on the nominal voltage and the network earthing system (TN or TT). This article focuses on the effectiveness of ADS in home installations (400/230 V) originally built in the TN–C earthing system.

The TN–C system is a three-phase low-voltage (LV) network in which the neutral point (N) of the supply transformer is directly earthed and the ECPs are metallically connected to this point. The protective-neutral conductor (PEN), connecting the ECPs with the N point of the transformer, is both a protective conductor and an active (neutral) conductor. It is earthed at multiple points and cannot be interrupted by any switches. The cross-section of the PEN conductor must meet the generally known criteria and should be the same as the cross-section of the phase conductors (for cross-sections up to 16 mm^2). In Poland, the TN–C system in home installations was already recommended in the regulations of 1960 [6], replaced in the early 1990s by the regulation [7] and the Polish standard [8], which was a translation of the IEC 60364 standard. The regulations [7,8] introduced the requirement that the minimum cross-section of the PEN conductor should be equal to 10 mm^2 of copper or 16 mm^2 of aluminum, which resulted in the abandonment of the TN–C system in home installations. However, considering that approximately 6 million residential units were built in Poland between 1960 and 1990 [9], and that their number currently stands at 16 million [10], it can be estimated that TN–C systems still constitute up to 40% of electrical installations in use (considering modernization and decommissioning of facilities). Furthermore, the so-called grandfather clause [11] does not oblige the replacement of TN–C installations with installations of a different system (e.g., TN–S) unless the building undergoes major reconstruction.

The TN–C system has two main drawbacks. The first is the violation of the single-fault condition principle, which states that a single fault should not cause a shock hazard [12]. Unfortunately, in this case, a break in the PEN conductor creates a hazard consisting of the appearance of a dangerous voltage at the ECPs, with no response from the protective devices. The second drawback is the inability to use residual current devices (RCDs) [13]. Consequently, overcurrent devices are used to implement ADS.

In the TN–C system, the single-phase short-circuit loop consists entirely of conductors, so the short-circuit currents caused by basic insulation damage (L–PEN short-circuit) reach high values [14]. Therefore, in these installations ADS can be implemented by overcurrent devices, i.e., fuses or miniature circuit breakers (MCBs). According to the IEC 60364 standard [5], ADS in a TN–C system is effective when—in the case of a short circuit—the power supply is switched off within the required time. This condition is met if the single-phase (L–PEN) short-circuit current is at least equal to the current causing automatic tripping of the protection at the required time, while in home installations, the permissible time of ADS is 0.4 s. If this condition cannot be met (the power supply is

switched off after a longer time), it must be ensured that the touch voltages during the flow of the short-circuit current do not exceed the permissible values, i.e., 50 V. This information is essential, because it allows ADS protection to be considered effective also in situations where the short-circuit current is lower than the current, causing the protection to operate within the required time, provided that the touch voltages do not exceed the permissible value.

The technical solutions for ADS recommended by the IEC 60364 standard [5] ensure a sufficiently low level of risk of electric shock at an acceptable investment cost. Unfortunately, these requirements generally apply to newly constructed buildings. In older buildings, constructed during periods when different technical requirements were in force, the risk of electric shock may be greater. The main factors that cause a higher level of risk in electrical installations supplying older buildings include [15,16]: outdated wiring systems, insufficient electrical capacity, outdated switchboards and fuses, a lack of safety switches (RCDs), and improperly installed wiring etc. It should be assumed that as these facilities operate over time, this risk will increase if appropriate remedial actions are not taken. An additional factor that may increase the risk of electric shock is the change in the way that a building is supplied, involving the installation of converter-based photovoltaic (PV) sources and battery energy storage systems (BESSs) integrated with the main building's power supply system. As a result of the expansion of the power supply system, the typical consumer installation becomes a prosumer installation.

According to the IEC standard [17], a prosumer electrical installation (PEI) is a low-voltage electrical installation connected or not to a distribution network, able to operate with local power supplies and/or with local storage units. This standard defines three types of PEI:

- stand-alone—permanently not connected to a distribution network,
- grid-connected—intended for operating only when connected to a distribution network,
- islandable—intended for operating either being connected to a distribution network or being disconnected from the distribution network.

Of the three types of PEI mentioned above, the operation of an islandable PEI is the most complex, and requires an additional energy control system, a specific electrical installation design, and effective protection measures for each operating mode, including protection against electric shock as a result of indirect contact (ADS). The last-mentioned issue is the subject of analysis in this article.

In the grid-connected mode, the protection measures against electric shock as a result of indirect contact inside the islandable PEI rely on the connection to the distribution network. In this case, the ADS is based primarily on the short-circuit current flowing from the network. Additionally, after the loss of network supply local sources shall be automatically disconnected, and a detection of such a situation is specified by the appropriate grid code [18]. A transition of the islandable PEI to island mode can be realized automatically or intentionally. In both situations, an appropriate switching device is necessary [19]. In island mode, voltage and frequency shall be regulated by a grid-forming converter [20], e.g., the bidirectional inverter of a BESS. This capability allows it to synchronize another source, e.g., PV microinstallation, and create a multi-source island. However, if the prosumer installation was not designed to operate while disconnected from the network (island mode), traditional protective measures against electric shock (ADS) inside the installation may not be effective in this case [21]. In particular, this situation may arise when older TN–C systems, designed solely for network supply, are converted into islandable PEI systems without being retrofitted into a TN–S earthing system. This is not in accordance with standard [17] but is encountered in practice.

According to several studies on PV operation and maintenance, [22–24] the greatest risk of electric shock in a PEI is posed by the improper installation of components; however, in general, the overall risk remains low, and it is relatively easy to eliminate. In turn, the probability of electric shock as a result of indirect contact in PEI grows over time and is mostly connected with the failure of RCDs [25]. In the first year of PEI operation this probability is equal to 1.97×10^{-4} whereas after 20 years it grows to 3.04×10^{-3}. The effectiveness of ADS in a PEI is also influenced by the type of RCD used [26]. All these observations are valid provided that an RCD was used in the PEI to implement ADS. However, as mentioned above, in a TN–C system it is not possible to use an RCD, and ADS is implemented using overcurrent devices.

The operation of overcurrent protection devices (fuses or MCBs) within the time specified by standard [5] requires that the current that flows through these devices be at least several times greater (5–7 times) than their rated current. This may cause a serious problem with the effectiveness of ADS in PEI during island operation, because in this mode the only sources of short-circuit currents are the inverters of the BESS and PV microinstallation. The value of the short-circuit current as well as its duration depends on the applied converter control scheme [27], but normally, in the event of a short circuit, PV and BESS inverters limit their maximal output current to a value only slightly higher (1.2–2 times) than the rated current [28]. Consequently, it is infeasible for power electronic converters with current-sensitive semiconductor devices to replicate the short-circuit behavior of the power network [29], which influences the operating conditions of overcurrent protection devices. The actual contribution of converter-based sources to the short-circuit current may be verified during adequate on-site measurements. Therefore, special attention is paid to this aspect in this paper.

The issue of the effectiveness of ADS during island operation of a PEI was analyzed in the article [30]. This paper examined the so-called collective PEI, consisting of several residential consumers (loads only) connected to the same public LV network and sharing one common energy storage unit and set of local power supplies (wind turbine and PV). The LV network was of the TN–C type, while the building's electrical installation was of TN–S type. Fuses (gG tripping characteristic) and MCBs (B characteristic) were used in the network and building installations, respectively. Short-circuit currents were calculated using the method described in the standard [30]. The obtained results proved that MCBs installed in internal installations of buildings provide effective protection against electric shock, whereas fuses do not ensure the effectiveness of ADS at every point of the network.

The analyses described in [30] concerned the island operation of collective PEIs with a relatively high capacity of BESS and generation sources. Such a microgrid configuration made it possible to achieve short-circuit currents of a magnitude similar to those flowing from the LV network. However, the situation will be different for an individual PEI equipped with a PV source and a BESS unit of significantly lower capacities. In this case, during island operation, the short-circuit currents will generally be substantially lower than during on-grid operation, which may affect the effectiveness of ADS. A detailed literature review reveals that there are no studies addressing the issue of the effectiveness of ADS in individual islandable PEI built in the TN–C earthing system and protected solely with overcurrent devices. Since such systems operate in practice, and their numbers are likely to grow as BESSs become more widespread, this should be regarded as a significant research gap, particularly as this issue concerns the safety of people using such installations in everyday life.

This article focuses on the effectiveness of ADS in an islandable PEI, equipped with converter-based PV source and a BESS, in various operating modes. The case study is an older residential building in which the installation was originally built in a TN–C earthing

system and ADS is implemented using overcurrent devices (fuses and MCBs). The main aim of the article is to analyze the effectiveness of this protection measure (ADS) under various power supply configurations of the building installation, in both grid-connected and island (off-grid) modes. The major contributions of this paper can be summarized as follows:

- the effectiveness of ADS in the various operating modes of the islandable PEI developed on the basis of a residential building installation operating in the TN–C earthing system was assessed using calculation and measurement methods,
- the applied methods confirmed that ADS is effective in all on-grid operating modes of the reference PEI, while contrary conclusions were obtained for island (off-grid) operation modes,
- measurements of short-circuit currents and touch voltage waveforms were taken to unambiguously assess the effectiveness of the ADS during actual short circuits occurring in the reference PEI,
- the results of waveform measurements showed that the requirements for protection against electric shock in the case of indirect contact (ADS) were met in all operating modes of the analyzed PEI,
- in on-grid modes, shock protection is provided by automatic disconnection of the grid supply by appropriate overcurrent protection, followed by automatic shutdown of the PV and BESS by their internal anti-islanding protections,
- in island (off-grid) modes, protection is provided by the automatic shutdown of the grid-forming source (BESS) by its internal overload protection, and of the PV source by its anti-islanding protection.

The remainder of this study is organized as follows. In Section 2, the reference PEI selected as a case study, as well as the methods used to assess the effectiveness of ADS, are briefly described. Section 3 presents the results of calculations and measurements, including those taken during actual short circuits, while Section 4 discusses the obtained results. Finally, the main conclusions are presented in Section 5.

2. Materials and Methods

2.1. Materials—Case Study (Reference PEI)

The conducted research assessed the effectiveness of ADS in a typical Polish residential building. A building from the early 1980s was chosen as a case study. The power supply of this building was made in accordance with the regulations in force in Poland at that time. This installation is made of copper conductors as a three-phase TN–C system. The internal power line has a cross-section of 4 mm^2, while the remaining wires have a cross-section of 1.5 mm^2. The protection system uses fuses with gG characteristics and rated currents of 25 A (main protection) and 16 A (load circuit protection). A few years ago, a PV micro-installation with a total power of 5.25 kW, connected with a three-phase 6 kVA inverter was installed in the building. According to the manufacturer's data, the rated current and maximum output current of the PV inverter are 8.7 A and 9.6 A, respectively.

Later, the building was additionally equipped with a BESS with a rated capacity of 20.8 kWh. This storage system consists of a BMS (Battery Management System) module, eight $LiFePO_4$ cells with a rated capacity of 2.6 kWh, and a three-phase bidirectional inverter with a rated power of 5.5 kVA (5 kW). In on-grid operation, the rated current and maximum output current of this inverter are 7.2 A and 7.9 A, whereas in off-grid operation, these currents are 7.2 A and 15.2 A respectively. The PV source and the BESS were connected to the building's existing power supply system using a 2.5 mm^2 copper cable operating in a TN–S configuration. Additionally, a 15 Ω grounding resistance was in-

stalled in the vicinity of the split point of the PEN conductor into separate N and PE conductors. Circuit breakers with a B characteristic and a rated current of 16 A were used to provide overcurrent protection for the PV source and BESS. The diagram of the installation (further called the reference PEI) is shown in Figure 1.

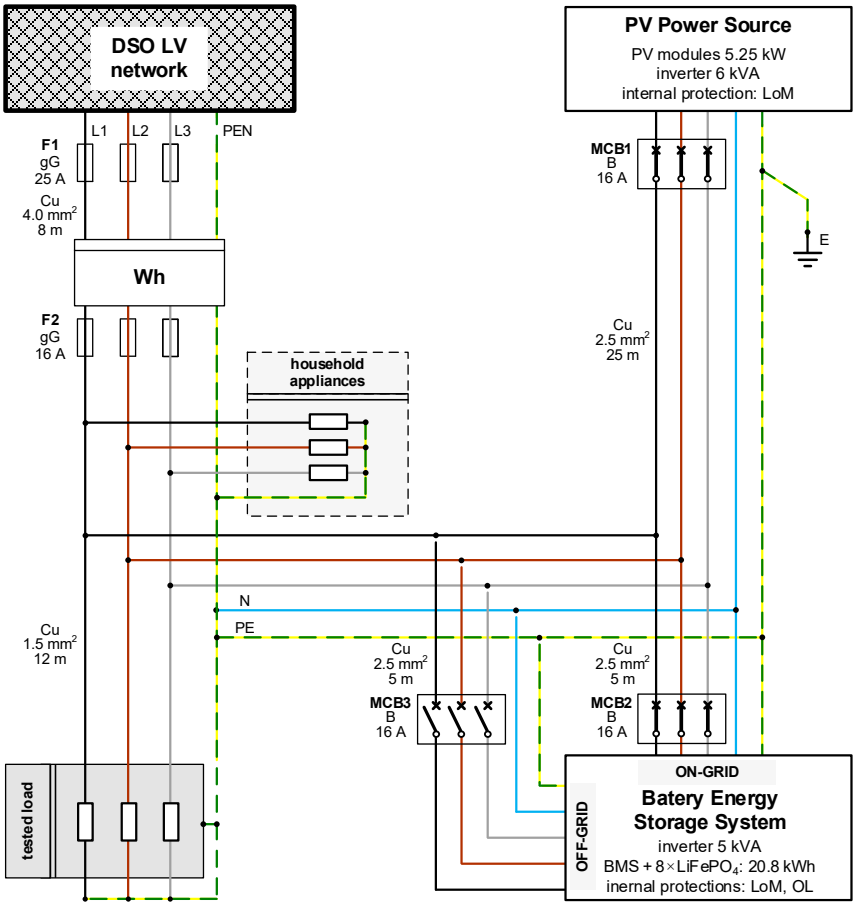


Figure 1. Schematic diagram of the power supply installation in the analyzed residential building equipped with a PV source and a BESS (reference PEI); internal protections: LoM—Loss of Mains, OL—Overload.

The considered residential building (reference PEI) is connected to an overhead-cable LV network operating in the TN–C earthing system, supplied by a transformer with a 15.75/0.4 kV/kV ratio and a rated power of 400 kVA. This transformer supplies five feeders, as shown in Figure 2 (the transformer is marked with a large red square). The longest feeder (overhead) supplies electricity to single-family residential buildings, while the remaining feeders (cable) supply multi-family residential buildings or commercial and service buildings (all customers are marked with a lightning bolt symbol). Eight customers with PV micro-installations with a total power of 35 kW are connected to the feeder supplying the single-family buildings (these customers are highlighted in the diagram with a yellow lightning bolt symbol). This feeder also includes one BESS, located in the reference PEI, marked with a red frame in Figure 2.

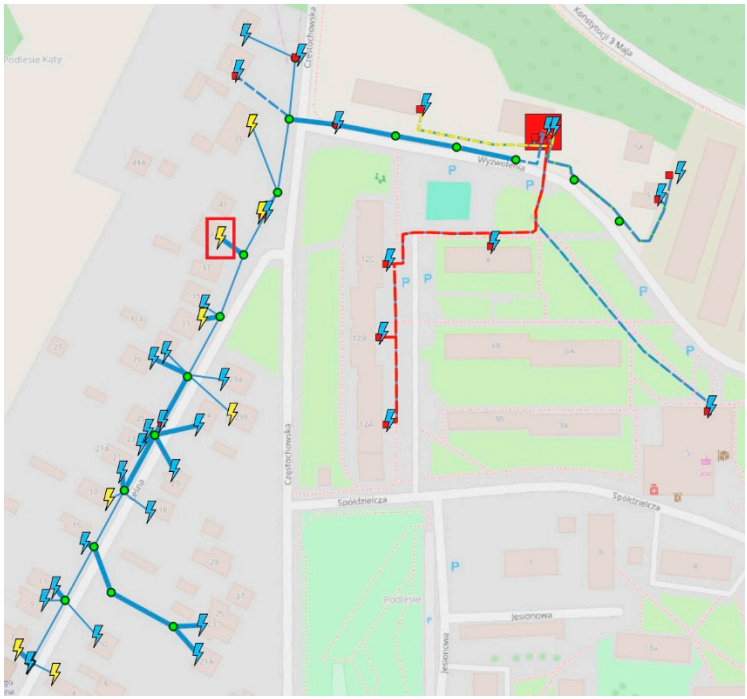


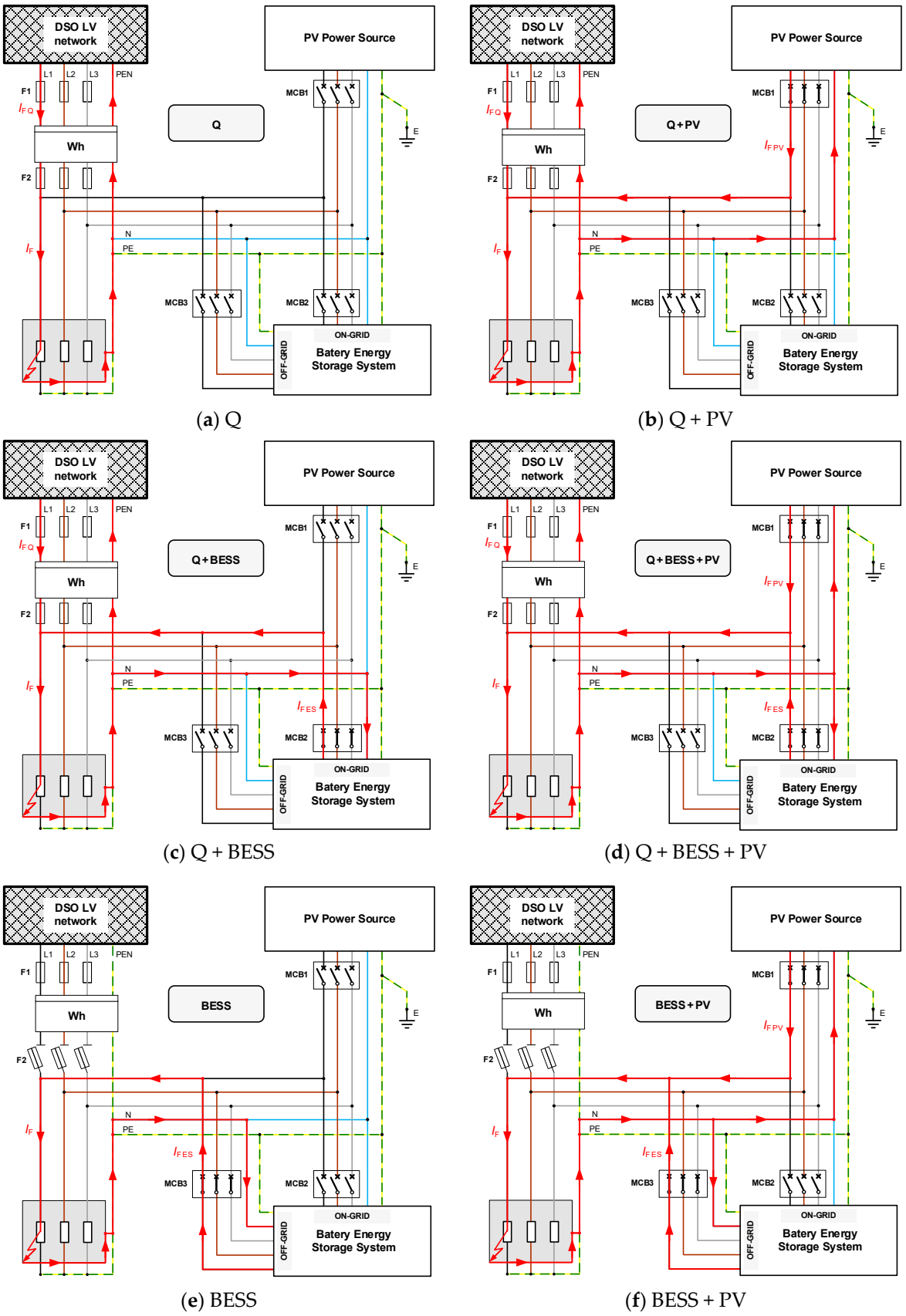
Figure 2. Diagram of the LV network supplying the reference PEI.

The primary operating mode of the reference PEI is parallel operation with the LV network (on-grid). This mode also allows for operation with a PV micro-installation and BESS, as shown in Figure 1. The BESS also enables island (off-grid) operation of the reference PEI, both with and without a PV source. Switching to island operation requires effective isolation of the reference PEI from the LV supply network, which is accomplished manually by removing the fuse links protecting the load circuits (the fuses F2 shown in Figure 1) and changing the position of the BESS's overcurrent protection contacts in the ON-GRID (MCB2 in Figure 1) and OFF-GRID (MCB3 in Figure 1) circuits. Therefore, the analyzed reference PEI allows for six different operating modes:

(a) power supply solely from the LV distribution network (Q),
(b) power supply from the LV network and PV (Q + PV),
(c) power supply from the LV network and BESS (Q + BESS),
(d) power supply from the LV network, BESS, and PV (Q + BESS + PV),
(e) power supply solely from the BESS (BESS),
(f) power supply from the BESS and PV (BESS + PV).

The operating modes listed above are schematically presented in Figure 3. This figure also shows the short-circuit current flow during an L-PEN fault.

In the following sections, the effectiveness of ADS in all operating modes of the reference PEI will be assessed using two commonly applied methods. Then, short-circuit currents and touch voltage waveforms will be measured to verify the effectiveness of ADS during actual short circuits.



(**a**) Q (**b**) Q + PV

(**c**) Q + BESS (**d**) Q + BESS + PV

(**e**) BESS (**f**) BESS + PV

Figure 3. Operating modes of the reference PEI with the marked L-PEN short-circuit current flow.

2.2. Methods for Assessing the Effectiveness of ADS

ADS is implemented by disconnecting the circuit in which the primary insulation of the receiver has been damaged. In a TN–C system, overcurrent protective devices (fuses

or MCBs) can be used as disconnecting devices [5]. ADS is effective if a resistance-free short circuit of any phase conductor L with the PEN conductor causes a short-circuit current flow at least equal to the current that causes the nearest protection (in the direction of the power supply) to trip automatically within the required time. This general condition can be expressed by the inequalities:

$$I_F \geq I_a \quad (1)$$

or

$$\frac{U_0}{Z_s} \geq I_a \quad (2)$$

where

I_F—single-phase (L–PEN) short-circuit current, in A,
I_a—current causing automatic tripping of the protection at the required time, in A,
U_0—network nominal voltage (versus earth), in V,
Z_S—fault loop impedance, in Ω.

The current I_a is read from the time-current characteristic of the protective device for the required disconnection time (0.4 s in a TN–C system) [5]. Figure 4 shows the time-current characteristics of the protective devices that are intended to implement ADS in the analyzed reference PEI (gG 16 A fuses or B16 A MCBs). The currents I_a for these elements are 100 A and 80 A, respectively (red solid line). Condition (1) or (2) should be met for a short circuit located at the furthest point of the protected circuit. When assessing the effectiveness of ADS in a PEI, the short-circuit current flowing through the analyzed protection devices in each PEI operating mode should be considered (see Figure 3). This issue will be discussed later in this article.

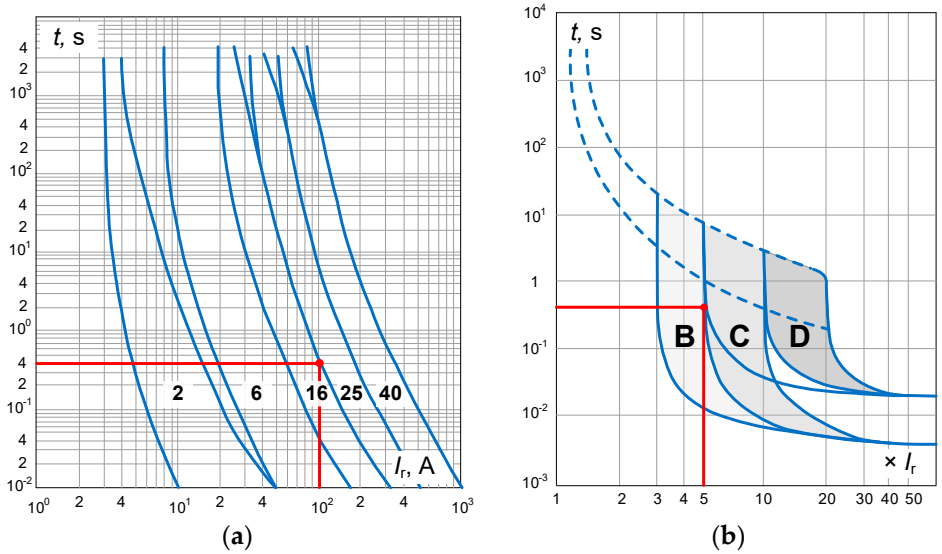


Figure 4. Time-current characteristics of the protective devices intended to implement ADS in the reference PEI: (**a**) gG 16 A-type fuses, (**b**) B16-type MCBs (own elaboration based on [14]).

As mentioned earlier, if switching off the power supply within the time required by standard [5] is not possible (it is executed after a longer time), protection against indirect contact is ensured if the touch voltages on the ECPs do not exceed the long-term permissible values, i.e., if the following condition is met:

$$U_T \leq U_L, \quad (3)$$

where:

U_T—touch voltage, in V,
U_L—permissible continuous touch voltage, equal to 50 V [5].

In practice, assessing the effectiveness of ADS using condition (1) or (2) is performed by determining the value of the fault loop impedance, which is used to calculate the expected value of the fault current. If these conditions are not met, the effectiveness of the protection should be verified using condition (3). The above steps can be performed using the calculation or measurement methods described in the following sections.

2.2.1. Calculation of Single-Phase Short-Circuit Current and Touch Voltage

Standard [31] and the literature [32] recommend calculating the single-phase short-circuit currents (which form the basis for assessing the effectiveness of ADS in electrical installations) using the following formula:

$$I_F = \frac{3\,cU_0}{\left|\underline{Z}_1 + \underline{Z}_2 + \underline{Z}_0\right|}, \quad (4)$$

where:

c—a voltage factor, taken as 0.9 or 1.1 for the calculation of the minimum or maximum short-circuit current, respectively,
$\underline{Z}_1$, $\underline{Z}_2$, $\underline{Z}_0$—symmetrical components of the short-circuit impedance, in Ω.

However, using the simplifying assumptions [32], the single-phase short-circuit current can be calculated using the formula:

$$I_F \approx \frac{cU_0}{\left|\underline{Z}_T + \underline{Z}_L + \underline{Z}_{PE}\right|}, \quad (5)$$

where:

$\underline{Z}_T$—transformer impedance, in Ω,
$\underline{Z}_L$—phase wire impedance, in Ω,
$\underline{Z}_{PE}$—return conductor impedance (PE or PEN), in Ω.

Standard [31] gives us only a very general clue about fault calculations in the systems with converters. According to it, the power station with a full-size converter, e.g., a PV system or a BESS, is modeled by a current source whose current value depends on the type of short circuit and must be provided by the manufacturer. This method of modeling PV and BESS operating in the reference PEI was adopted in this article. The values of currents emitted by these sources during a short circuit were assumed to be their maximum output currents given in Section 2 (a limitation of this approach is that it neglects transient phenomena which affect the short-circuit current value during the initial phase, as will be demonstrated later in the article). It was also assumed that PV sources installed at other prosumers supplied by the same transformer are the sources of short-circuit current of a negligible magnitude compared with the value of the short-circuit current originating from the transformer and therefore they were neglected in the calculations. Taking into account these assumptions, Figure 5 shows the equivalent diagrams for calculating the single-phase short-circuit current in the event of an L–PEN short circuit in various operating modes of the reference PEI.

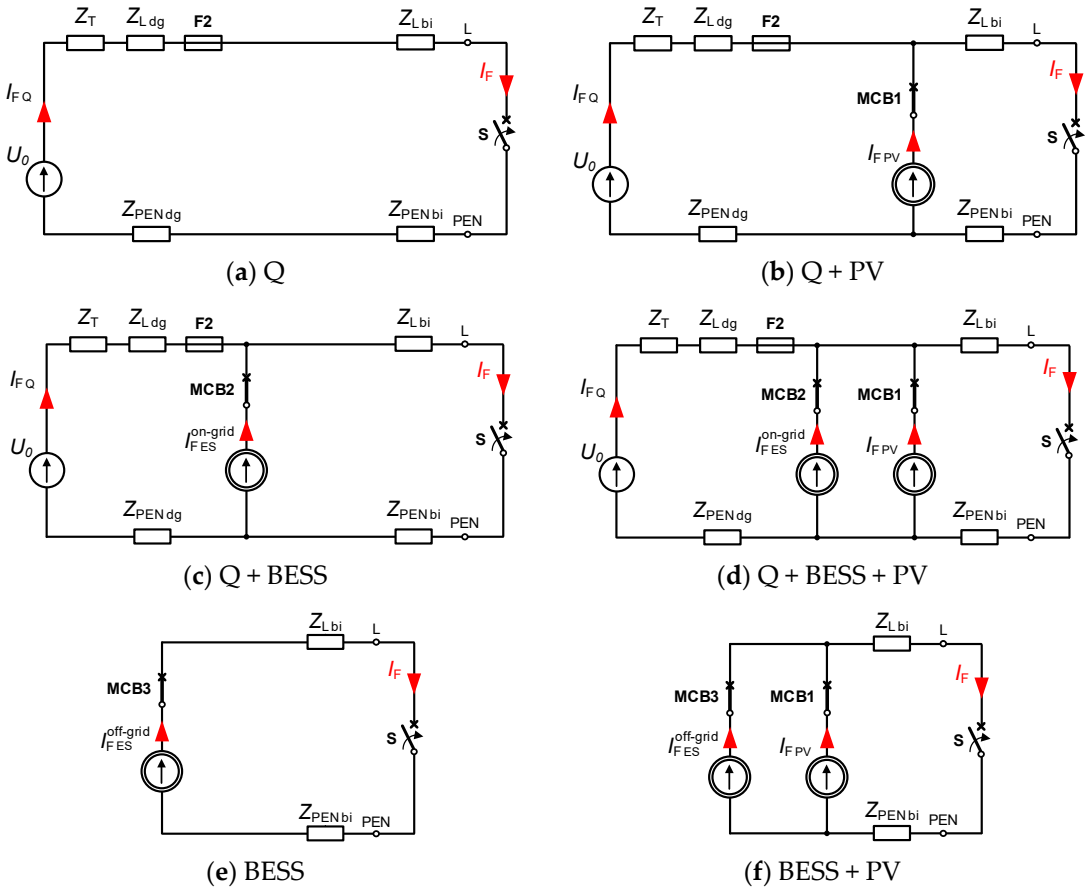


Figure 5. Equivalent diagrams for calculating the single-phase short circuit current in the event of an L–PEN short-circuit in various operating modes of the reference PEI.

The relevant standard [33] requires that, for the purpose of verifying the effectiveness of ADS, the calculated minimum (c = 0.9) single-phase short-circuit current must be further reduced by multiplying the short-circuit loop impedance by a safety factor k equal to 1.5 (to eliminate the effect of temperature on the active component of the short-circuit loop impedance and the phase error of the fault loop impedance meters). This approach has been adopted in this article. In turn, the maximum single-phase short-circuit current (c = 1.1, k = 1) was used to calculate the touch voltage. Considering all the indicated assumptions, the simplified formula for calculating the single-phase short-circuit current in the case of supplying the reference PEI solely from the LV distribution network (Q) is as follows:

$$I_{F\,Q} = \frac{cU_0}{k\left|\underline{Z}_T + \underline{Z}_{L\,dg} + \underline{Z}_{L\,bi} + \underline{Z}_{PEN\,dg} + \underline{Z}_{PEN\,bi}\right|}, \quad (6)$$

while the formulas for calculating these currents in various operating modes of the reference PEI are presented in Table 1.

Table 1. Formulas for calculating the single-phase short-circuit current (I_F) in the event of a L–PEN short-circuit in various operating modes of the reference PEI.

Operating Mode of PEI	Formula	
Q	$I_F = I_{F\,Q}$	(7)
Q + PV	$I_F = I_{F\,Q} + I_{F\,PV}$	(8)
Q + BESS	$I_F = I_{F\,Q} + I_{F\,ES}^{on\text{-}grid}$	(9)

Q + BESS + PV	$I_F = I_{F\,Q} + I_{F\,ES}^{\text{on-grid}} + I_{F\,PV}$	(10)
BESS	$I_F = I_{F\,ES}^{\text{off-grid}} \ (I_{F\,Q} = 0)$	(11)
BESS + PV	$I_F = I_{F\,ES}^{\text{off-grid}} + I_{F\,PV} \ (I_{F\,Q} = 0)$	(12)

Based on the calculated maximum values of single-phase short-circuit currents, the touch voltage in each operating mode of the reference PEI can be determined using the following formula:

$$U_T = I_{F\,Q}\, Z_{PEN\,dg} + I_F\, Z_{PEN\,bi}. \quad (13)$$

2.2.2. Measurement of Fault Loop Impedance and Touch Voltage

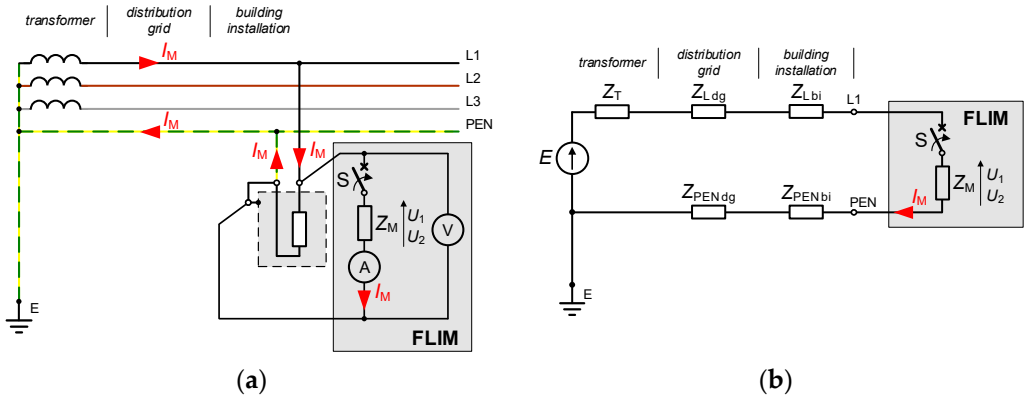
The most common method of measuring fault loop impedance uses the so-called artificial short circuit through the measuring impedance [34]. An exemplary measuring circuit for home installation supplied solely from the LV network is shown in Figure 6a, while the equivalent circuit diagram is shown in Figure 6b. The measurement involves a short-term connection of the impedance of a known value to the circuit (instead of the receiver), which generates a controlled current pulse, allowing the fault loop impedance to be determined without tripping the protection devices. The measured value of the fault loop impedance is determined using the formula:

$$Z_s = \frac{\Delta U}{I_M} = \frac{U_1 - U_2}{\frac{U_2}{Z_M}} = Z_M\left(\frac{U_1}{U_2} - 1\right), \quad (14)$$

where

U_1, U_2—voltages measured before and after closing switch S, respectively, in V,
I_M—measuring current, in A,
Z_M—measuring impedance, in Ω.

The measurement is typically performed using a specialized Fault Loop Impedance Meter (FLIM). Based on the measured fault loop impedance values, the prospective fault current is determined and compared to the current causing automatic tripping of the protection at the required time, which verifies condition (2). If this condition is not met, the touch voltages at the ECPs should be measured.



(**a**) (**b**)

Figure 6. Principle of fault loop impedance measurement: (**a**) a connection of the fault loop impedance meter (FLIM) in the TN–C system, and (**b**) an equivalent of the tested circuit.

When measuring touch voltages, similarly to the measurement of fault loop impedance, an artificial short circuit through the impedance is also made and the voltage between the ECP and the ground (measuring electrode) is measured during this short circuit

[35] (Figure 7a). The equivalent circuit of this system is shown in Figure 7b. The touch voltage U_T occurring during an actual short circuit between the L and PEN conductors is calculated using the formula:

$$U_T = \frac{U_M}{I_M} I_F = \frac{U_M}{I_M} \frac{U_0}{Z_S}, \quad (15)$$

where:

U_M—voltage measured after closing switch S, in V.

The measurement is usually performed by using a specialized Touch Voltage Meter (TVM).

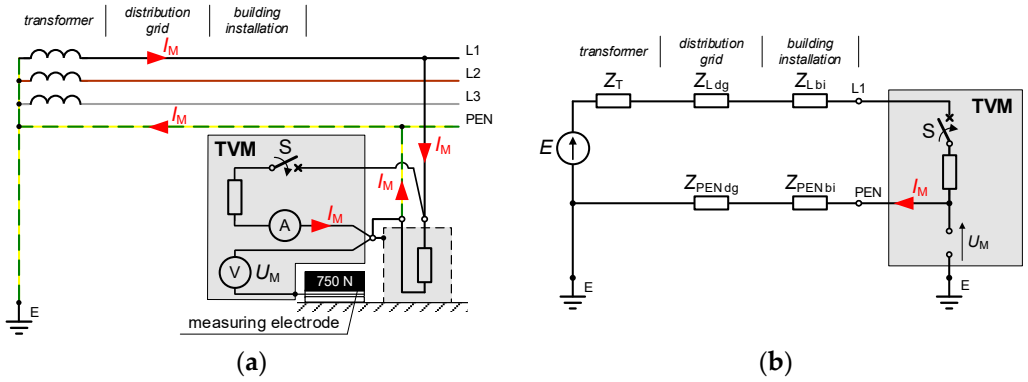


Figure 7. Principle of touch voltage measurement: (**a**) connection of the touch voltage meter (TVM) in the TN–C system, (**b**) equivalent of the tested circuit.

3. Results

3.1. Calculation of Single-Phase Short-Circuit Current and Touch Voltage

To calculate the short-circuit currents and touch voltages for the purpose of verifying the effectiveness of ADS in the event of an L–PEN short circuit in various operating modes of the reference PEI, the simplified formulas given in Table 1 were used. The following parameters for the transformer and wiring were adopted for calculating their impedances (only the resistances of individual components are considered in the calculations):

- transformer:
  rated power 400 kVA, load losses 1.05%, LV rated voltage 0.4 kV,
- LV distribution grid:
  Section 1—type YAKY 120 mm², conductivity 33 MS/m, length 39 m,
  Section 2—type AsXSn 70 mm², conductivity 33 MS/m, length 116 m,
  Section 3—type Al 50 mm², conductivity 33 MS/m, length 73 m,
  Section **4**—type AsXSn 16 mm², conductivity 33 MS/m, length 14 m,
- building installation:
  Section 1—copper wire 4 mm², conductivity 55 MS/m, length 8 m,
  Section 2—copper wire 1,5 mm², conductivity 55 MS/m, length 12 m.

The resulting values of resistances are summarized in Table 2.

Table 2. Resistances (R) of individual components of the fault loop of the reference PEI for the calculation of short-circuit currents and touch voltages (reactive parts of impedances are neglected).

Element	Transformer	LV Distribution Grid			Building Installation		
		Sect. 1	Sect. 2	Sect. 3	Sect. 4	Sect. 1	Sect. 2
R, Ω	0.0042	0.0098	0.0502	0.0442	0.0265	0.0364	0.1455
Partial sum of R, Ω	0.0042		0.1307			0.1819	

The calculations of short-circuit currents were carried out both for the safety factor k = 1.5 (in accordance with standard [33] to verify whether the overcurrent protection of a TN–C system would be effectively triggered), and for k = 1 (to calculate touch voltages with an appropriate safety margin). In both cases, the appropriate value of the factor c was used. For example, in a situation where the reference PEI is operating while powered solely from the LV distribution network (with the BESS and PV switched off), the minimum single-phase short-circuit current is:

$$I_{\mathrm{F\,min}} = \frac{0.9U_0}{1.5|\underline{Z}_{\mathrm{T}}+\underline{Z}_{\mathrm{dg}}+\underline{Z}_{\mathrm{bi}}+\underline{Z}_{\mathrm{PEN\,dg}}+\underline{Z}_{\mathrm{PEN\,bi}}|} = \frac{0.9\cdot 230}{1.5\cdot(0.0042+2\cdot(0.1307+0.1819))} = 219.3\ \mathrm{A}, \quad (16)$$

while the maximum single-phase short-circuit current is equal to:

$$I_{\mathrm{F\,max}} = \frac{1.1U_0}{|\underline{Z}_{\mathrm{T}}+\underline{Z}_{\mathrm{dg}}+\underline{Z}_{\mathrm{bi}}+\underline{Z}_{\mathrm{PEN\,dg}}+\underline{Z}_{\mathrm{PEN\,bi}}|} = \frac{1.1\cdot 230}{0.0042+2\cdot(0.1307+0.1819)} = 402.0\ \mathrm{A}. \quad (17)$$

If, during a short circuit, the reference PEI is supplied by other sources (BESS and PV), the maximum currents of these sources are added directly to the short-circuit current flowing from the grid, treating PV and BESS as current sources. The results of the single-phase short-circuit current calculations are summarized in Table 3. In turn, Figure 8 shows the comparison of the minimum single-phase short-circuit current and the current causing automatic tripping of the overcurrent protection (100 A and 80 A) at the required time in various operating modes of the reference PEI.

Table 3. Calculated values of the minimum ($I_{\mathrm{F\,min}}$) and maximum ($I_{\mathrm{F\,max}}$) single-phase short-circuit current in the event of L–PEN short-circuit in various operating modes of the reference PEI.

Operating Mode of PEI	$I_{\mathrm{F\,min}}$, A (c = 0.9, k = 1.5)	$I_{\mathrm{F\,max}}$, A (c = 1.1, k = 1)
Q	219.3	402.0
Q + PV	228.9	411.6
Q + BESS	227.2	409.9
Q + BESS + PV	236.8	419.5
BESS	15.2	15.2
BESS + PV	24.8	24.8

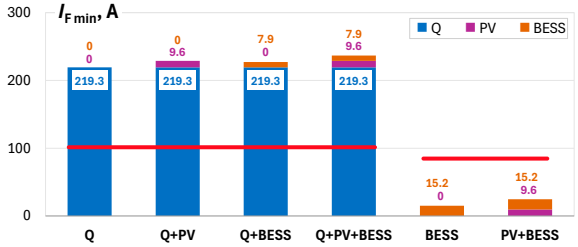


Figure 8. Calculated values of the minimum single-phase short circuit current and their comparison with the current causing automatic tripping of the overcurrent protection devices at the required time (red line) in various operating modes of the reference PEI.

Figure 8 shows that in all situations where the LV grid is involved in a short circuit, ADS can be considered effective. In these cases, the (gG 16 A) fuse F2 shown in Figure 1 is intended to implement ADS, and the calculated minimum short-circuit current flowing from the grid exceeds the trip threshold of this protection device (100 A). After the loss of network supply local sources (PV and BESS) in the reference PEI shall be automatically disconnected (the circuit breakers MCB1 and MCB2 will not operate). However, in the island modes (supplying the reference PEI from BESS or BESS and PV), the overcurrent

protection devices MCB1 and MCB3 will not respond correctly as the short-circuit currents flowing from the BESS and PV are much lower than their trip threshold (80 A). For this reason, the expected values of touch voltage were calculated in the next step. For completeness, touch voltages were determined for all operating modes of the reference PEI, even though this was not necessary when powered from the LV grid.

As the permissible touch voltage must not be exceeded under the worst-case safety conditions, the expected touch voltages were calculated using the maximum short-circuit current presented in Table 3. Formula (13) was used. For example, when the reference PEI is powered solely from the LV grid, the touch voltage at the furthest ECP is:

$$U_T = I_{F\,Q}\, Z_{PEN\,dg} + I_F\, Z_{PEN\,bi} = 402.0 \cdot 0.1307 + 402.0 \cdot 0.1819 = 125.7\ \text{V}. \quad (18)$$

The results of the touch voltage calculations are summarized in Table 4.

Table 4. Calculated values of touch voltages (U_T) in the event of an L–PEN short-circuit in various operating modes of the reference PEI.

Operating Mode of PEI	U_T, V
Q	125.7
Q+ PV	127.4
Q + BESS	127.1
Q + BESS + PV	128.8
BESS	2.8
BESS + PV	4.5

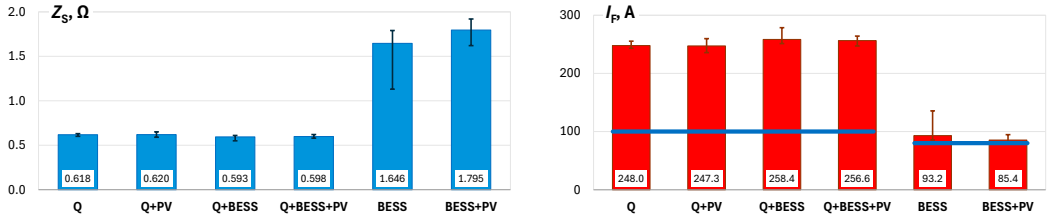
The obtained values indicate that in all operating modes of the reference PEI in which the short circuit is supplied from the LV network, the touch voltages on the ECPs exceed the permissible value (50 V). Nevertheless, as shown earlier, ADS is effective in these cases, as the basic condition (1) is satisfied. In island modes (supplying the reference PEI from the BESS and PV or BESS) condition (1) is not met; however, in these cases, the touch voltage does not exceed the safe limit, so there is no risk of electric shock (under normal conditions).

3.2. Measurement of Fault Loop Impedance

Fault loop impedance measurements were performed in each phase of the reference PEI. The artificial short-circuit method described in Section 2.2.2 was applied, and FLIM (Sonel MPI 525) with a 10 Ω measuring resistance was used. The FLIM was connected to the installation socket, which is the furthest from the primary power source (LV network). Twelve measurements were taken for each phase. The measurements were performed in four series, with the fault loop impedance measured three times in each case. The measurements were made on different days and at different times of the day (including nights) during normal use of electrical appliances in the building. During the fault loop impedance measurements in PEI island operation, the load on the PV and BESS inverters exceeded 50% of their rated power [36] (except PV load during the night measurements).

Figure 9a shows the average values of the measured fault loop impedance in various operating modes of the reference PEI (the phase with the highest measured impedance was selected). The highest and lowest measured impedance values were also marked for each average result. Based on the measured fault loop impedance values and considering the safety factor $k = 1.5$ [33], the expected short-circuit current was calculated. The calculated current values were compared with the current values (100 A and 80 A) causing automatic tripping of the protection at the required time for the overcurrent protection devices installed in the reference PEI (see Figure 4). This comparison is presented in Figure 9b. In each operating mode of the reference PEI power supply, condition (1) was generally

met, allowing ADS to be considered effective. Therefore, touch voltage measurements were not performed.



(**a**) (**b**)

Figure 9. Measured values of fault loop impedance (Z_S) (**a**) and calculated values of short-circuit current (I_F) and their comparison with the current causing automatic tripping (I_a) of the overcurrent protection at the required time (blue line) (**b**) in various operating modes of the reference PEI.

3.3. Measurement of Short-Circuit Currents and Touch Voltage Waveforms in the Reference PEI During Actual L-PEN Short Circuits

The results of the commonly used calculation (Section 3.1) and measurement (Section 3.2) methods indicated that, when operating on-grid, ADS is effective in the reference PEI. In these cases, the short-circuit current flowing from the LV network will trigger the appropriate protection (fuse F2 in the reference PEI) within the required time. After the loss of supply from the network, the PV and BESS should be automatically switched off by their internal anti-islanding protections. In turn, the results obtained for off-grid operation do not allow for the formulation of clear conclusions regarding the effectiveness of ADS. In these cases, the calculation method indicates that the MCBs implementing ADS will not operate within the required time due to too low a value of the short-circuit current flowing from the BESS and PV, while the measurement of the fault loop impedance indicates that ADS will be effective. Therefore, to unambiguously assess the possibility of electric shock in the event of indirect contact in various operating modes of the reference PEI, this section describes the results of measurements carried out during actual L-PEN short circuits in this system (two short-circuit tests were performed for each scenario).

Measurement recordings were taken for all operating modes of the reference PEI, as shown in Figure 3. The current (i_{Fx}) waveforms during short circuits and the corresponding touch voltage (u_T) waveforms were measured and recorded. Measuring probe connections are displayed in Figure 10 (the voltage probe was positioned outside the building, approximately 40 m away, in an area free from any other underground installations). Selected views of the measurements taken at the test site are shown in Figure 11. The specifications of the measuring equipment used are provided in Table 5. For each case, the waveform of the measured quantity was recorded by means of a digital oscilloscope (position 2 in Table 5). The fault condition was triggered based on the rising edge of the short-circuit current (i_{Fx}). The oscilloscope time base was set in such a way as to record the entire course of the fault condition. The length of the recording was 100,000 samples. The results of the experiment were recorded as oscilloscope screenshot graphic files and stored on a USB drive in the form of CSV data. Based on these data, Figures 12 and 13 were prepared.

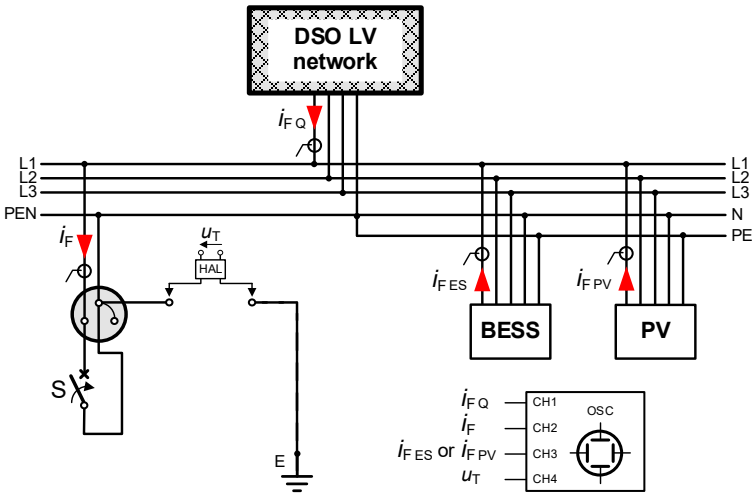


Figure 10. Diagram of a circuit for measuring short-circuit currents and touch voltage waveforms in the reference PEI during actual short circuits.

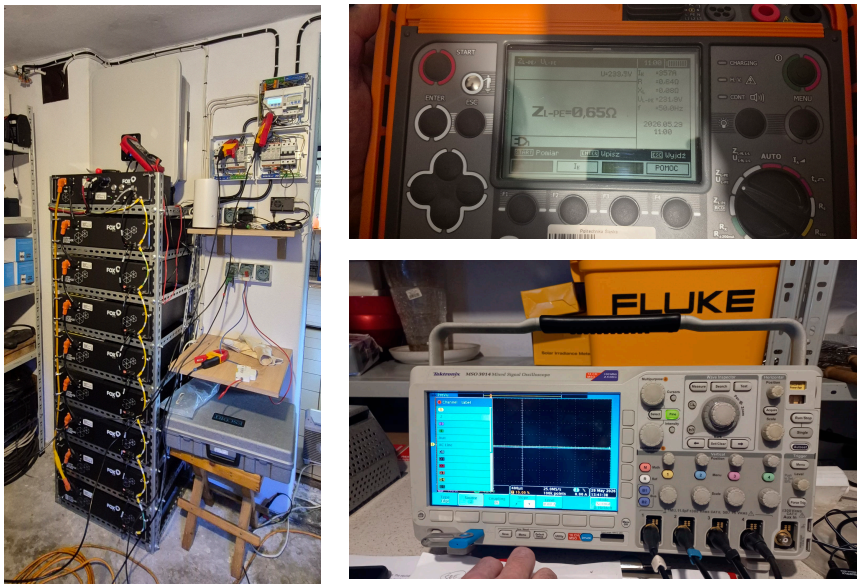
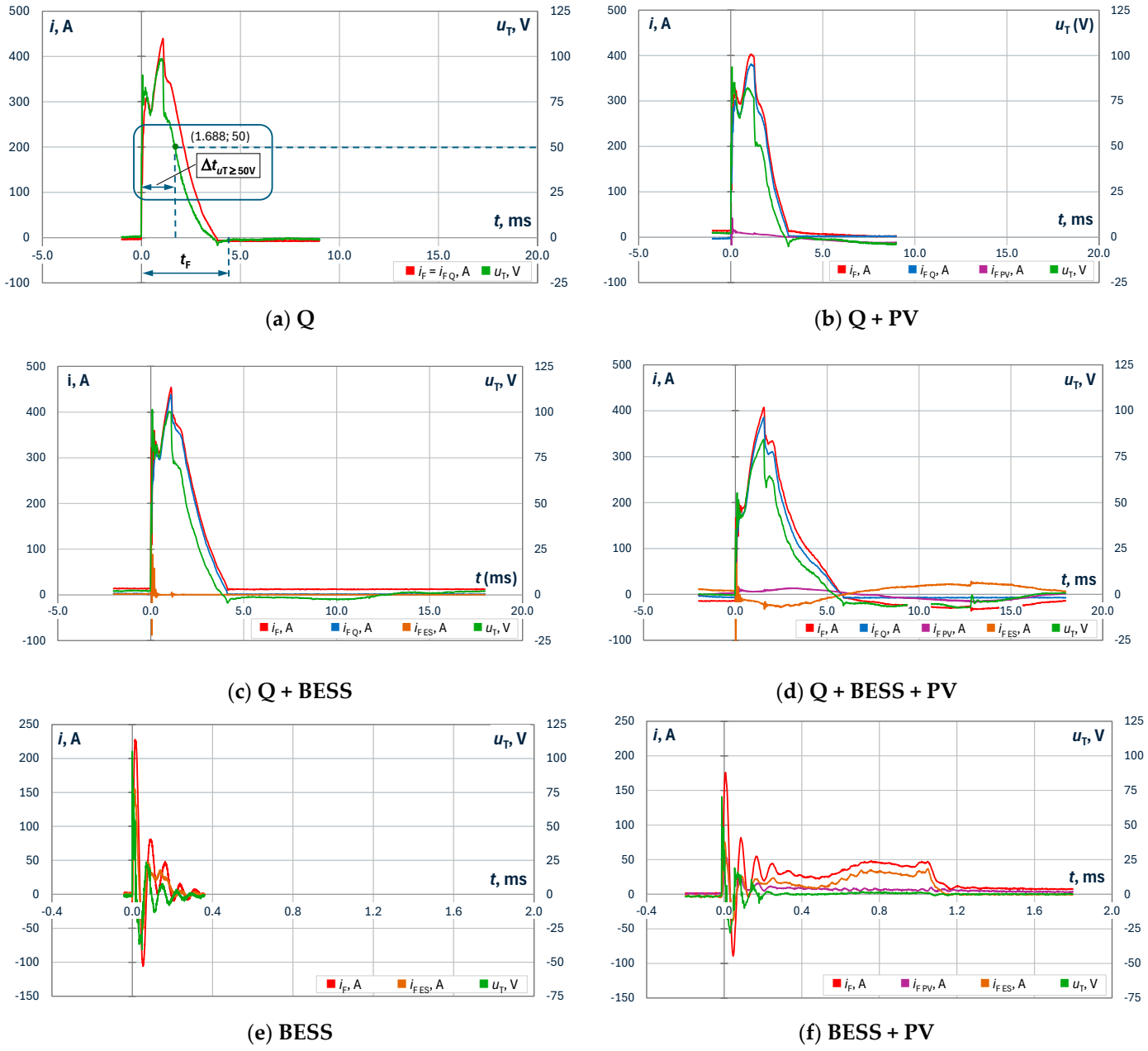


Figure 11. Selected views of measuring equipment and facilities of the reference PEI.

In Figures 12 and 13 the waveforms of the instantaneous values of the short-circuit current (resultant current i_F and currents flowing from individual sources $i_{F\,Q}$, $i_{F\,PV}$ and $i_{F\,ES}$) as well as the touch voltage u_T recorded during the measurements are shown (Figure 12a also shows how the short-circuit duration t_F is determined). In Table 6, the maximum and minimum values of these parameters are given. This table also shows the time interval $\Delta t_{uT\geq 50V}$, which corresponds to the occurrence of a touch voltage over 50 V (this time interval is measured from fault inception up to the time point when the touch voltage u_T decreases below 50 V—see Figure 12a). In turn, Table 7 shows the operation of overcurrent protections in the installation (F2, MCB1, MCB2 and MCB3) as well as the internal protections of the BESS and PV (anti-islanding—LoM and overcurrent—OL) in the event of failure for all considered operating modes of the reference PEI.

Table 5. Measuring equipment specification.

No.	Measuring Equipment	Quantity
1.	FLIM: SONEL MPI 525, range 0…19.99 Ω, accuracy ±6%	1
2.	Digital oscilloscope: Tektronix MSO 3014, bandwidth 100 MHz, sampling rate 2.5 GS/s, record length 100 kpoints	1
3.	Current clamp probe: FLUKE i400s, bandwidth DC ÷ 25 MHz, range 400 A, 1 mV/A, accuracy 2% + 0.04 A (45 Hz do 400 Hz),Ch.1 ÷ 3	3
4.	Voltage differential probe: PINTEK DP-25, attenuation ×200, bandwidth DC…25 MHz, accuracy 2%, Ch.4	1



(**a**) **Q**

(**b**) **Q + PV**

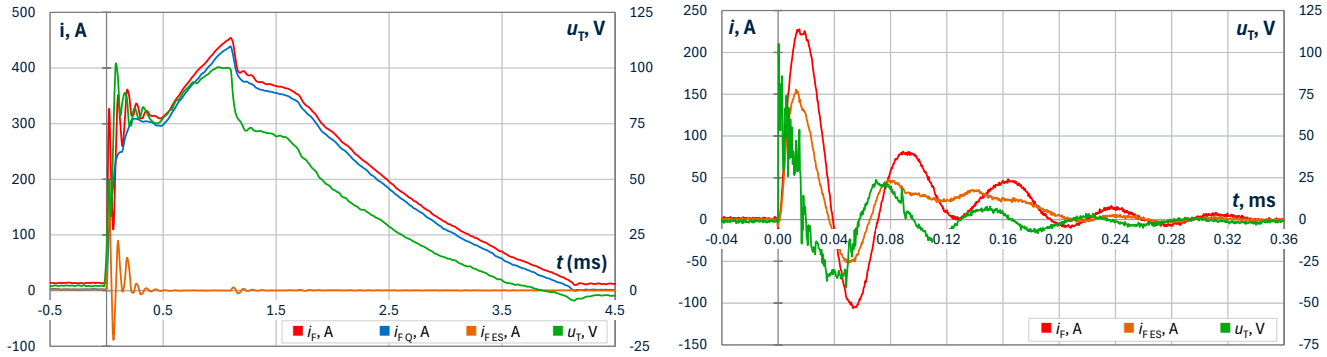
(**c**) **Q + BESS**

(**d**) **Q + BESS + PV**

(**e**) **BESS**

(**f**) **BESS + PV**

Figure 12. Short-circuit currents and touch voltage waveforms measured during actual short circuits in various operating modes of the reference PEI.



(a) Q + BESS—zoom of Figure 12c **(b) BESS—zoom of Figure 12e**

Figure 13. Short-circuit currents and touch voltage waveforms measured during actual short circuits in selected operating modes of the reference PEI—zoomed-in views showing greater details.

Table 6. Selected parameters of short-circuit currents and touch voltage waveforms measured during actual short circuits in various operating modes of the reference PEI—acc. to Figure 12 and 13.

Operating Mode of PEI	Extreme Value	i_F, A	$i_{F\,Q}$, A	$i_{F\,PV}$, A	$i_{F\,ES}$, A	u_T, V	$\Delta t_{uT\geq 50V}$, ms
Q	max	439.7	439.7	-	-	98.8	1.688
	min	−8.6	−8.6	-	-	−4.3	
Q + PV	max	402.9	381.5	75.6	-	93.8	1.622
	min	0.8	−3.8	−24.1	-	−5.1	
Q + BESS	max	454.2	438.5	-	196.2	101.4	1.903
	min	10.2	0.3	-	−87.9	−4.5	
Q + BESS + PV	max	407.3	385.4	37.4	68.9	84.4	2.219
	min	−35.9	−8.2	−16.6	−124.7	−7.4	
BESS	max	227.8	-	-	155.5	105.2	0.015
	min	−105.9	-	-	−52.8	−40.6	
BESS + PV	max	176.0	-	53.7	75.9	70.5	0.011
	min	−89.4	-	−18.0	−38.3	−27.9	

Table 7. Operation of protective devices in considered operating modes of the reference PEI.

Operating Mode of PEI	F2	MCB1	MCB2	MCB3	LoM.BESS	OL.BESS	LoM.PV
Q	☒	–	–	–	–	–	–
Q + PV	☒	☐	–	–	–	–	☒
Q + BESS	☒	–	☐	–	☒	☐	–
Q + BESS + PV	☒	☐	☐	–	☒	☐	☒
BESS	–	–	–	☐	☐	☒	–
BESS + PV	–	☐	–	☐	☐	☒	☒

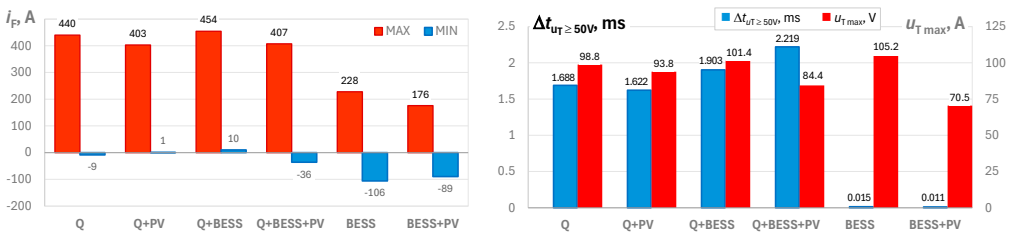
☒—operation successful. ☐—operation unsuccessful. –—circuit disconnected. LoM—Loss of Mains (anti-islanding internal protection of BESS and PV). OL—Overload (overcurrent internal protection of BESS).

All recorded waveforms are characterized by dynamic changes in the measured parameters (both current and voltage) at the initial moment of the short circuit. Depending on the case being tested, the duration of transient phenomena (accompanying the short circuit) ranges approximately from 0.5 ms to 5 ms. In all on-grid modes (Q+), ADS in the reference PEI was realized by fuse F2. In each of these cases, fuse F2 tripped on a short

circuit as expected (current $i_{F\,Q}$ was large enough to blow fuse F2). In cases with the PV source and the BESS connected, their overcurrent protections (MCB1 and MCB2, respectively) did not trip (the currents $i_{F\,PV}$ and $i_{F\,ES}$ were too small to trigger this breakers), but the PV source and BESS automatically switched off after detecting off-grid operation. This behavior is confirmed in the case of Q + BESS (Figure 12c), while in the cases of Q + PV (Figure 12b) and Q + BESS + PV (Figure 12d) such a trip did not occur during the recording. However, based on the analysis of the error logs recorded by the PV and BESS converters, it was found that both units were switched off by their internal anti-islanding protections. This means that the delay in the operation of this protection may last longer than the largest registration interval of 18 ms.

In island (off-grid) modes, the reference PEI was adequately reconfigured (Figure 3e,f). In these cases, the BESS was the leading (grid-forming) source, while the PV inverter operated in grid-following mode, as it would when the grid was connected. The recorded waveforms (Figure 12e,f) have a clearly oscillatory character. Furthermore, the components of the short-circuit current do not balance with the resultant short-circuit current: $i_F \neq i_{F\,ES}$ and $i_F \neq i_{F\,ES} + i_{F\,PV}$. This situation is caused by the discharge of capacitance of the input filter of the PV and BESS converters, as well as the household appliances connected to the reference PEI during the measurements. In island modes, the MCB3 circuit breaker was intended to provide ADS; however, due to the insufficient fault current $i_{F\,ES}$, this protection did not trip. This means that in off-grid modes, this overcurrent device did not provide shock protection. However, the BESS control system quickly identified the fault condition and disconnected the power supply. In both cases (BESS, BESS + PV), the measured time interval $\Delta t_{uT\geq 50V}$ was very short and equal to 0.015 ms and 0.011 ms, respectively (Table 6).

The graphs (Figure 14) compare the recorded maximum and minimum short-circuit current i_F (Figure 14a), the time interval $\Delta t_{uT\geq 50V}$, and the maximum touch voltage u_T (Figure 14b). The highest peak value of the short-circuit current (above 400 A) occurred in the following modes: Q + BESS, Q, Q + BESS + PV, and Q + PV, respectively, with the difference between the latter two systems being very small. The lowest peak value of the short-circuit current (below 250 A) was generated in the BESS and PV + BESS cases, respectively. Figure 14b shows that the peak value of the touch voltage u_T did not exceed 110 V and dropped permanently to a value below 50 V in a very short time ($\Delta t_{uT\geq 50V}$ for all tested modes did not exceed 2.5 ms). The voltage value above 50 V persisted for the longest time in the Q + BESS + PV system (2.219 ms), and for the shortest time in the BESS and BESS + PV systems (0.015 ms and 0.011 ms, respectively).



(**a**) (**b**)

Figure 14. Comparison of selected parameters for the tested operating modes: extreme values of the instantaneous short-circuit current i_F (**a**), the time interval $\Delta t_{uT\geq 50V}$ of the occurrence of the touch voltage u_T above 50 V (**b**) and the maximum value of the instantaneous touch voltage $u_{T\,max}$ (**b**).

4. Discussion: An Assessment of the Effectiveness of ADS in Various Operating Modes of the Reference PEI

The investigations described in the previous sections of this paper aimed to assess the effectiveness of electric shock protection in the event of indirect contact (ADS). They were conducted in a reference PEI (described in Section 2.1), which was created based on the electrical installation of a residential building, originally constructed in a TN–C earthing system and now equipped with a PV source and a BESS. The tests were conducted for various modes of operation of the reference PEI, including on-grid operation (Q, Q + PV, Q + BESS, and Q + PV + BESS modes) and island operation (BESS and BESS + PV modes). First, the effectiveness of ADS was assessed using calculation and measurement methods (described in Section 2.2) widely used in design and operational practice.

For the reference PEI supplied exclusively from the network (Q), good consistency was achieved between the calculated value of the short-circuit current and the value determined on the basis of the fault loop impedance measurement (Figures 8 and 9b). Both methods clearly demonstrated that in this mode ADS will be effective due to the high value of single-phase short-circuit current flowing from the grid. In this operating mode of the reference PEI, disconnection of the circuit in which the short circuit occurred will be achieved by the operation of overcurrent protection with an appropriately selected time-current characteristic and rated current (in the reference PEI this is the fuse F2, marked in Figure 1).

Both methods indicated that in modes where the tested PEI is additionally supplied by a PV source and energy storage (Q + PV, Q + BESS, and Q + PV + BESS), the effectiveness of ADS will also be ensured. This effectiveness of protection stems from the fact that in these cases, the component originating from the power system retains the dominant share of the short-circuit current. Consequently, the overcurrent protection at the LV grid connection (fuse F2 in the reference PEI) will again be responsible for disconnecting the faulted circuit. After this protection is triggered, the PV source and BESS should be disconnected by their internal anti-islanding protections; however, the overcurrent protection of these sources—circuit breakers MCB1 and MCB2 in Figure 1—will not be triggered.

A significantly different situation occurs during island operation of the reference PEI (BESS and BESS + PV modes). Analysis of the results presented in Figures 8 and 9b for these cases reveals significant discrepancies between the short-circuit current values determined using the calculation method and those determined based on fault loop impedance measurements. The consequence of these discrepancies is that the conclusions regarding the effectiveness of the ADS during off-grid operation of the reference PEI vary depending on the method used. In the case of the analytical method, this assessment is negative, because due to low short-circuit current values, the overcurrent protection devices will not automatically trip within the required time (in the reference PEI, MCB1 and MCB3 breakers, through which the short-circuit currents generated by the PV source and BESS flow, respectively—Figure 3e,f). For this reason, in the next step, the expected maximum touch voltage values at the ECPs during a short circuit were calculated. The obtained results (Table 4) indicate no shock hazard during PEI island operation, despite the failure of the appropriate overcurrent protection devices to trip. In the case of the method based on the fault loop impedance measurement result, the ADS effectiveness assessment is generally positive, as the determined short-circuit current value meets general condition (1). In particular, this assessment is unambiguous for the PEI supplied solely from the energy storage (BESS mode), because in this case the actual short-circuit current flows through the MCB3 protection (Figure 3e), and its value, calculated based on the measured fault loop impedance, is sufficient to trip the circuit breaker (MCB3) within the required time. However, doubts may arise regarding the result of this assessment for the BESS +

PV operation mode (Figure 3f). In this PEI operation mode, condition (1) is generally met, but a component of the calculated short-circuit current will flow through the PV source overcurrent protection (MCB1) and another component through the BESS protection (MCB3). However, based on the fault loop impedance measurement, it is not possible to calculate the values of these currents, and therefore determine whether these protection devices will trip within the required time. Furthermore, this method does not consider the actual behavior of power electronic converters during short circuits, including the operation of their internal protection and transient phenomena, which affect the short-circuit current value during the initial phase. Therefore, it can be concluded that assessing the effectiveness of ADS for PEI island operation by measuring fault loop impedance is inappropriate, because traditional fault loop impedance meters are not suitable for measurements in systems powered by sources with power electronic converters.

The methods used to assess the effectiveness of ADS for the reference PEI operating in island mode (BESS and BESS + PV modes) did not allow for a clear assessment of the behavior of the analyzed system during short circuits. Therefore, to ultimately assess the effectiveness of ADS and the possibility of the appearance of touch voltage causing a shock hazard, measurements of short-circuit currents and touch voltages waveforms were conducted during actual single-phase short circuits in the system. For completeness, these tests were performed for all operation modes of the reference PEI.

Measurements of current and voltage waveforms during actual short circuits demonstrated the effectiveness of shock protection in all operating modes of the reference PEI. During on-grid operation, shock protection in the event of indirect contact was ensured by automatic tripping of the overcurrent protection at the connection to the distribution grid (fuse F2, marked in Figure 1). After its tripping, the remaining sources (PV and BESS) operating in grid-following mode were disconnected by the anti-islanding protection of their converters, while their overcurrent protections located in the PEI (MCB1 and MCB2 circuit breakers) were not activated. In turn, during island operation, initiated short circuits caused tripping of the internal overload protection of the grid-forming source converter (BESS), and then the anti-islanding protection of the PV source converter (operating in grid-following mode relative to the BESS). In these cases, none of the overcurrent protection devices for these sources in the installation (MCB1 and MCB3 circuit breakers) tripped during the short-circuit tests. It should be noted, however, that although the short-circuit currents generated by the PV source and BESS were insufficient to ensure the operation of these protection devices within the required time, the shock hazard during a short circuit was minimal, as the touch voltages (peak values) appearing on the ECPs exceeded 50 V for no longer than 0.02 ms (according to standard [37], for a short-circuit duration of 40 ms, the touch voltage may reach 500 V (RMS value).

The conducted research demonstrated the advantage of the measurement method (measurements of the current and voltage waveforms during actual faults) over conventional methods of assessing the effectiveness of ADS (calculation of short-circuit currents and measurements of fault loop impedance). Conventional methods allow only for the estimation of the effective value of short-circuit currents (when measuring fault loop impedance, without indicating the current flow in the PEI when several sources are in operation) and touch voltages, while recording the waveforms of these quantities enables the analysis of their actual instantaneous values during transient states. This is particularly important for PEIs containing sources with power electronic converters, whose behavior during disturbances is largely determined by their control and protection algorithms.

It should be noted that the scope of the conducted research was limited by the lack of access on the detailed data of converters used in the reference PEI, especially regarding their control and protection functions (particularly functional details regarding the inverter's internal overload protection are not disclosed by the manufacturer; however, for

the reference PEI, it can be stated that the inverter's documentation and its nameplate indicate full compliance with the relevant standards [38,39]). At this stage of research, this prevented the development of an accurate simulation model of the system that would allow for the reproduction of experimentally obtained waveforms. In future work, the authors are considering developing models of individual PEI elements, considering the recorded measurement waveforms, and then creating a complete PEI model for various operating modes. Such a model could be using, among other applications, to analyze fault states, which would allow for the proposal of new methods for assessing the effectiveness of shock protection in installations containing sources with power electronic converters.

5. Conclusions

Based on the results described in the article, it can be generally concluded that although the analyzed reference PEI based on a TN–C earthing system is not compliant with the applicable standards, it can still provide effective protection against electric shock in the case of indirect contact, both in on-grid and off-grid operation. However, this requires the cooperation of several protective devices, both within the installation itself and within the power electronic converters built into the PV and BESS.

In on-grid operation modes, it must be ensured that the overcurrent protection installed at the LV grid connection effectively implements ADS, and that the anti-islanding protection of the local power sources operating in grid-following mode (e.g., PV, BESS) effectively disconnects these units after the power supply from the grid is disconnected. In island (off-grid) operation modes, the grid-forming source (e.g., BESS) must have reliable internal overload protection that will effectively shut down this source in the event of a short circuit. After the grid-forming source is disconnected, the remaining sources operating in grid-following mode within this island will be disconnected by their anti-islanding protection. These aspects should be considered during the design, construction and operational inspections of PEIs.

Author Contributions: Conceptualization, R.K., M.K., P.K., A.L., K.M., B.W., D.D., A.D., H.K. and T.R.; methodology, R.K., M.K., P.K., A.L., K.M., B.W., D.D., A.D., H.K. and T.R.; validation, R.K., M.K., P.K., A.L., K.M., B.W., D.D., A.D., H.K. and T.R.; formal analysis, R.K., M.K., P.K., A.L., K.M., B.W., D.D., A.D., H.K. and T.R.; investigation, R.K., M.K., P.K., A.L., K.M., B.W., D.D., A.D., H.K. and T.R.; resources, R.K., M.K., P.K., A.L., K.M., B.W., D.D., A.D., H.K. and T.R.; data curation, R.K., M.K., P.K., A.L., K.M., B.W., D.D., A.D., H.K. and T.R.; writing—original draft preparation, R.K., M.K., P.K., A.L., K.M., B.W., D.D., A.D., H.K. and T.R.; writing—review and editing, R.K., M.K., P.K., A.L., K.M., B.W., D.D., A.D., H.K. and T.R.; visualization, R.K., M.K., P.K., A.L., K.M., B.W., D.D., A.D., H.K. and T.R.

Funding: This research received no external funding.

Data Availability Statement: Data (measurement results) available on demand.

Conflicts of Interest: The authors declare no conflicts of interest.

Nomenclature

The following symbols are used in this manuscript:

c	a voltage factor, taken as 0.9 or 1.1 for the calculation of the minimum or maximum short-circuit current, respectively,
E	equivalent voltage source, in V,
I_a	current of automatic tripping of the protection at the required time, in A,
I_F	single-phase (L–PEN) short-circuit current, in A,

$I_{F\,ES}$	single-phase short-circuit current flowing from BESS in on-grid and off-grid operating mode, respectively, in A,
$I_{F\,min}$	minimum value of single-phase short-circuit current, in A,
$I_{F\,max}$	maximum value of single-phase short-circuit current, in A,
$I_{F\,PV}$	single-phase short-circuit current flowing from PV source, in A,
$I_{F\,Q}$	single-phase short-circuit current flowing from LV network (Q), in A,
I_M	measuring current, in A,
I_r	rated current, in A,
i_x	instantaneous value of fault current from x-type of source, in A,
k	safety factor in accordance with the standard [33],
R	resistances of individual components of the fault loop, in Ω,
t	time, in s or ms,
t_F	short-circuit duration, in ms,
$\Delta t_{uT\geq 50V}$	time interval during which the touch voltage u_T exceeds 50 V, in ms,
U_0	network nominal voltage (versus earth), in V,
U_1, U_2	voltages measured before and after closing the switch S, respectively, in V,
U_L	permissible continuous touch voltage, equal to 50 V,
U_M	voltage measured after closing the switch S, in V,
U_T, u_T	touch voltage, RMS and instantaneous values, respectively, in V,
ΔU	voltage difference, in V,
Z_0, Z_1, Z_2	symmetrical components of the short-circuit impedance, in Ω,
Z_L	phase wire impedance, in Ω,
$Z_{L\,bi}$	phase wire impedance of building installation, in Ω,
$Z_{L\,dg}$	phase wire impedance of distribution grid, in Ω,
Z_M	measuring impedance, in Ω,
Z_{PE}	return conductor impedance (PE or PEN), in Ω,
$Z_{PEN\,bi}$	PEN wire impedance of building installation, in Ω,
$Z_{PEN\,dg}$	PEN wire impedance of distribution grid, in Ω,
Z_S	fault loop impedance, in Ω,
Z_T	transformer impedance, in Ω.

Abbreviations

The following acronyms are used in this manuscript:

ADS	Automatic Disconnection of Supply,
BESS	Battery Energy Storage System,
BMS	Battery Management System,
CSV	Comma-Separated Values file format,
ECP	Exposed Conductive Part,
F	Fuse,
FLIM	Fault Loop Impedance Meter,
IEC	International Electrotechnical Commission,
L	line (phase) wire/conductor,
LoM	Loss of Mains, anti-islanding internal protection of converter,
L–PEN	line to PEN circuit, single-phase circuit,
LV	low-voltage,
MCB	Miniature Circuit Breaker,
N	neutral point, neutral (active) conductor,
OL	overload protection, overcurrent internal protection of converter,
OFF-GRID	BESS operating in island mode (grid-forming),
ON-GRID	BESS (or PV) operating in grid-connected mode (grid-following),
PE	protective conductor,
PEI	Prosumer Electrical Installation,
PEN	protective-neutral conductor,
PV	photovoltaic source,

https://doi.org/10.3390/en19235764

Q	network/grid feeder connection point, network/grid feeder,
RCD	Residual Current Device,
TN, TN–C, TN–S, TT	various LV grid earthing systems,
TVM	Touch Voltage Meter,
USB	Universal Serial Bus communication standard.

References

1. Eurostat. Energy Consumption in Households. Available online: https://ec.europa.eu/eurostat/statistics-explained/index.php?title=Energy_consumption_in_households (accessed on 10 March 2026).
2. Fish, R.M.; Geddes, L.A. Conduction of electrical current to and through the human body: A review. *Eplasty* **2009**, *9*, e44.
3. Dąda, A.; Błaut, P.; Miller, P. Selected network systems and protection against electric shock in the light of new standards and regulations. In Proceedings of the 2019 Progress in Applied Electrical Engineering (PAEE), Koscielisko, Poland, 17–21 June 2019; pp. 1–6. https://doi.org/10.1109/PAEE.2019.8789003.
4. Mitolo, M.A.G. *Electrical Safety of Low-Voltage Systems*; McGraw-Hill Companies: New York, NY, USA, 2009.
5. *IEC 60364-4-41*; Consolidated Version (IEC 60364-4-41:2005+AMD1:2017 CSV). Low Voltage Electrical Installations—Part 4-41: Protection for Safety—Protection Against Electric Shock.
6. Order of the Minister of Mining and Energy of 20 April 1960 on Regulations Concerning the Construction of Electrical Installations. M.P. 1960 nr 38 poz. 190. Available online: https://isap.sejm.gov.pl/isap.nsf/DocDetails.xsp?id=WMP19600380190 (accessed on 9 April 2026). (In Polish)
7. Regulation of the Minister of Industry of 8 October 1990 on the Technical Requirements to Be Met by Electrical Equipment with Regard to Protection Against Electric Shock. Dz.U. 1990 nr 81, poz. 473. Available online: https://isap.sejm.gov.pl/isap.nsf/DocDetails.xsp?id=WDU19900810473 (accessed on 9 April 2026). (In Polish)
8. *PN-E-05009-41:1992P*; Electrical Installations of Buildings. Protection for Safety. Protection Against Electric Shock. (In Polish)
9. Ciok, S.; Ilnicki, D. *Spatial and Time Diversity of Housing Construction in Poland*; Committee for Spatial Economy and Regional Planning, Polish Academy of Sciences, Studia KPZK: Warsaw, Poland, 2018; Volume 183. Available online: https://journals.pan.pl/dlibra/publication/123590/edition/107803/content (accessed on 9 April 2026). (In Polish)
10. Statistics Poland: The Housing Market in 2024. Key Insights. Available online: https://stat.gov.pl/files/gfx/portalinformacyjny/pl/defaultaktualnosci/5492/14/8/1/gospodarka_mieszkaniowa_w_2024_r.pdf (accessed on 8 May 2026). (In Polish)
11. Musiał, E. Understanding Regulations and Standards. Biul. SEP INPE, 2007, no 93-94. Available online: www.edward-musial.info/pliki/pojmowanie_przepisow_norm.pdf (accessed on 12 April 2026). (In Polish)
12. Musiał, E. Protection Against Electric Shock in IT, TT and TN Systems. Interaction Between Two Different Systems Within a Single Installation. Biul. SEP INPE, 2013, no 162-163. Available online: http://www.edward-musial.info/pliki/ochrona_it_tt_tn.pdf (accessed on 12 April 2026). (In Polish)
13. Zhang, X.; Liu, Y.; Han, Z.; Zhang, H. Enhancing Low-Voltage Distribution Network Safety through Advanced Residual Current Protection Techniques. *Appl. Sci.* **2024**, *14*, 3256. https://doi.org/10.3390/app14083256.
14. Czapp, S. *Ochrona przeciwporażeniowa w sieciach i instalacjach niskiego napięcia*, PWN: Warszawa, Poland, 2023. (In Polish)
15. Electrical Issues in Older Homes—Causes, Risks and Solutions. Available online: https://complete-connectrix.co.uk/electrical-issues-in-older-homes (accessed on 19 April 2026).
16. Common Electrical Risks in Older Homes and Buildings. Available online: https://buildinginstitute.edu.au/blog-details/common-electrical-risks-in-older-homes-and-buildings (accessed on 19 April 2026).
17. *IEC 60364-8-82:2022*; Low-Voltage Electrical Installations—Part 8-82: Functional Aspects—Prosumer's Low-Voltage Electrical Installations.
18. EUR-Lex. Commission Regulation (EU) 2016/631 of 14 April 2016 Establishing a Network Code on Requirements for Grid Connection of Generators. Available online: https://eur-lex.europa.eu/eli/reg/2016/631/oj (accessed on 21 April 2026).
19. IET. *Code of Practice for Electrical Energy Storage Systems*, 3rd ed.; 2024.
20. Hasan, M.M.; Razmi, D.; Babayomi, O.; Davidson, I.; Terzija, V.; Zhang, Z. Advanced control and protection strategies for grid-forming inverters in microgrids: A review. *Int. J. Electr. Power Energy Syst.* **2025**, *172*, 111297. https://doi.org/10.1016/j.ijepes.2025.111297.
21. Mazur, Ł.; Cieślik, S.; Czapp, S. Trends in Locally Balanced Energy Systems without the Use of Fossil Fuels: A Review. *Energies* **2023**, *16*, 4551. https://doi.org/10.3390/en16124551.

22. Sotiris, N.K.; Tsoutsos, T. Assessment of the safe operation and maintenance of photovoltaic systems. *Energy* **2015**, *93*, 1633–1638. https://doi.org/10.1016/j.energy.2015.10.037.
23. Dhanup, S.; Pillai, N.; Rajasekar. A comprehensive review on protection challenges and fault diagnosis in PV systems. *Renew. Sustain. Energy Rev.* **2018**, *91*, 18–40. https://doi.org/10.1016/j.rser.2018.03.082.
24. Osmani, K.; Haddad, A.; Lemenand, T.; Castanier, B.; Alkhedher, M.; Ramadan, M. A critical review of PV systems' faults with the relevant detection methods. *Energy Nexus* **2023**, *12*, 100257. https://doi.org/10.1016/j.nexus.2023.100257.
25. Ciric, R.; Håkedal, E.L.; Pedersen, O.T.; Dørum, K.O. Reliability and electrical safety of grid-connected household PV systems: Data-driven risk analysis and insights. *Smart Energy* **2025**, *18*, 100182. https://doi.org/10.1016/j.segy.2025.100182.
26. Czapp, S. Residual current devices in installations with PV energy sources. *Przegląd Elektrotechniczny* Volume 98, **2022**, 100–104. https://doi.org/10.15199/48.2022.12.25.
27. Haj-ahmed, M.A.; Illindala, M.S. The Influence of Inverter-Based DGs and Their Controllers on Distribution Network Protection. *IEEE Trans. Ind. Appl.* **2014**, *50*, 2928–2937. https://doi.org/10.1109/TIA.2013.2297452.
28. Chandra, A.; Singh, G.K.; Pant, V. Protection of AC microgrid integrated with renewable energy sources—A research review and future trends. *Electr. Power Syst. Res.* **2021**, *193*, 107036. https://doi.org/10.1016/j.epsr.2021.107036.
29. Liu, C.; Cai, X.; Li, R.; Yang, R. Optimal Short-circuit current control of the Grid-forming converter during grid fault condition. *IET Renew. Power Gener.* **2021**, *15*, 2185–2194. https://doi.org/10.1049/rpg2.12149.
30. Sobolewski, R.A.; Lis, R. Protection verification and designing while establishing collective prosumer's low-voltage electrical installation: A case study. *Electr. Power Syst. Res.* **2023**, *218*, 109185. https://doi.org/10.1016/j.epsr.2023.109185.
31. IEC 60909-0:2016. Short-Circuit Currents in Three-Phase a.c. Systems—Part 0: Calculation of Currents.
32. Markiewicz, H. *Electrical Installations*; WNT: Warsaw, Poland, 2018. (In Polish)
33. *IEC 60364-6:2016*; Low Voltage Electrical Installations—Part 6: Verification.
34. Czapp, S. Method of earth fault loop impedance measurement without nuisance tripping of RCDs in 3-phase low-voltage circuits. *Metrol. Meas. Syst.* **2019**, *26*, 128350. https://doi.org/10.24425/mms.2019.128350.
35. Corvino, A.; Maurella, A. Measurement of touch voltage in electrical installations, in TN system, in low voltage earth fault. In Proceedings of the 8th Mediterranean Electrotechnical Conference on Industrial Applications in Power Systems, Computer Science and Telecommunications (MELECON 96), Bari, Italy, 13–16 May 1996; Volume 3, pp. 1375–1378. https://doi.org/10.1109/MELCON.1996.551203.
36. Katarzyński, J.; Olesz, M. Fault Loop Impedance Measurement in Circuits Fed by UPS and Principle of Safety Protection. *Sustainability* **2020**, *12*, 10126. https://doi.org/10.3390/su122310126.
37. *PN-IEC-60364-4-442:1999*; Electrical Installations of Buildings. Protection for Safety. Protection Against Overvoltages. Protection of Low-Voltage Installations Against Temporary Overvoltages and Faults Between High-Voltage Systems and Earth.
38. *IEC 62109-2:2011*; Safety of Power Converters for Use in Photovoltaic Power Systems—Part 2: Particular Requirements for Inverters.
39. *EN 50549-1:2019*; Requirements for Generating Plants to Be Connected in Parallel with Distribution Networks—Part 1: Connection to a LV Distribution Network—Generating Plants Up to and Including Type B.

Disclaimer/Publisher's Note: The statements, opinions and data contained in all publications are solely those of the individual author(s) and contributor(s) and not of MDPI and/or the editor(s). MDPI and/or the editor(s) disclaim responsibility for any injury to people or property resulting from any ideas, methods, instructions or products referred to in the content.